Available online at www.sciencedirect.com
ScienceDirect
Catalysis Today 127 (2007) 17–30
CATALYSIS TODAY
www.elsevier.com/locate/cattod

Single-event microkinetics for coke formation during the catalytic cracking of (cyclo)alkane/1-octene mixtures

R. Quintana-Solórzano [a], J.W. Thybaut [a,*], P. Galtier [b], G.B. Marin [a]

[a] *Laboratorium voor Petrochemische Techniek, Ghent University, Krijgslaan 281, S-5, B-9000 Ghent, Belgium*
[b] *Institut Français du Pétrole, IFP Vernaison, BP n° 3, 69390 Vernaison, France*

Available online 1 May 2007

Abstract

A single-event microkinetic model (SEMK) is applied to model initial coking rates during the catalytic cracking of (cyclo)alkane/1-octene mixtures at 693–753 K and (cyclo)alkane and 1-octene inlet partial pressures of 26.6 and 4.8 kPa on a REUSY equilibrium catalyst. Three types of irreversible alkylations involving both gas phase and surface coke precursors, viz., alkylation of phenyl substituted carbenium ions with C_3–C_5 alkenes, alkylation of the nucleus of monoaromatics with C_3–C_5 alkylcarbenium ions, and alkylation of C_8–C_{10} alkylcarbenium ions with C_3–C_5 alkenes, have been considered as rate-determining steps in coke formation. The bulky alkylated species formed out of these alkylations are considered as coke. The activation energies for these alkylations obtained via non-isothermal regression are independent of the feedstock within the parameters confidence limits reflecting the fundamental character of the SEMK. The negative effect of temperature on the experimentally observed coking rates is qualitatively described and is explained in terms of an overcompensation of the increase of the rate coefficient by a lower surface coke precursor concentration.

Keywords: Catalytic cracking; Single-event microkinetics; (Cyclo)alkanes; Alkenes; Coke; Alkylation

1. Introduction

The catalytic cracking of heavy crude oil fractions is inevitably accompanied by catalyst deactivation due to coke formation. The zeolitic component of the catalyst, i.e., a Y-zeolite providing most of the cracking activity, is especially sensitive to deactivation by coke due to its acid properties and its micropores [1]. The coking rate and the corresponding catalyst activity decay together with the nature of the coke deposits are strongly linked to the hydrocarbons nature, operating conditions and catalyst properties [2].

The complexity of the reaction pathway to coke greatly depends on the hydrocarbon nature. An industrial feedstock is constituted of a very large number of compounds which can be classified in a limited number of hydrocarbon types, viz., alkanes, alkenes, cycloalkanes and (poly)aromatics [3]. For hydrocarbons belonging to the same family, both cracking and coking patterns are expected to be similar because the same elementary reactions are necessarily involved.

It is reported in the literature that (poly)aromatics and alkenes possess the highest coke selectivity, whereas alkanes and cycloalkanes exhibit the lowest [4]. The higher tendency of (poly)aromatics and alkenes to produce coke has been associated to their pronounced proton acceptor character. Although the coking process is complex, a limited number elementary reactions families can be identified, i.e., hydride transfers, alkylations, cyclisations, deprotonations. Bimolecular interactions between adsorbed carbenium ions and gas phase coke precursors have been found to play a very important role in coke formation and, hence, the catalyst surface coverage is a key parameter in the modeling of the coking phenomenon [5].

Traditionally the deactivating effect of coke on the catalyst activity is accounted for by means of the deactivation functions [6,7]. This requires the calculation of the coke content on the catalyst by means of kinetic expressions. Rather than a pure deactivating effect by coking, in practice an interaction occurs between the cracking and the coking reactions [8]. Recently, during the cracking of isobutene on ultra-stable Y-zeolites at relatively high coke levels, a positive effect of coke formation

* Corresponding author. Tel.: +32 9 264 4519; fax: + 32 9 264 4999.
E-mail address: Joris.Thybaut@UGent.be (J.W. Thybaut).

0920-5861/$ – see front matter © 2007 Elsevier B.V. All rights reserved.
doi:10.1016/j.cattod.2007.03.024

Nomenclature

A	aromatic or preexponential factor
$\tilde{A}$	single-event preexponential factor (s^{-1} or $(s\ kPa)^{-1}$)
A_{rep}	reparameterized preexponential factor(s^{-1} or $(s\ kPa)^{-1}$)
alk	alkylation
b	vector of kinetic parameters that minimized the objective function
buchex	*n*-butylcyclohexane
c(alk)	cyclo(alkane)
cO	cycloalkene
cycl	cyclisation
C_c	coke on catalyst ($kg_{coke}\ (kg_{cat})^{-1}$)
C_j^+	alkylcarbenium ions with j carbon atoms
C_{t,H^+}	concentration of acid sites on the catalyst ($mol\ (kg_{cat})^{-1}$)
dep	deprotonation
DA	diaromatic
E_{act}	activation energy ($kJ\ (mol)^{-1}$)
f	oscillating frequency (Hz)
$F^o_{c(alk)}$	cyclo(alkane) inlet molar flow rate $(mol(s)^{-1})$
htr	hydride transfer
$\tilde{k}_{alk\_side}$	single-event rate coefficient for (side) alkylation involved in coke ($mol_{coke}\ (s\ kPa)^{-1}$)
$\tilde{k}_{alk\_nucl}$	single-event rate coefficient for nucleus alkylation involved in coke ($mol_{coke}\ (s\ kPa)^{-1}$)
k_o	TEOM reactor spring constant ($kg\ (Hz)^2$)
$Mw_{c(alk)}$	cyclo(alkane) molecular mass
n_e	number of single events
n_{exp}	number of experiments
n_{step}	number of differential elements considered for the reactor
N	cycloalkane
N^+	cyclic carbenium ion
Pp	partial pressure
PCP	protonated cyclopropane intermediates
prot	protonation
r^o_c	initial coking rate ($kg_{coke}\ (kg_{cat}\ s)^{-1}$)
$(r^o_c)_{alk\_side}$	initial coking rate via nucleus alkylation reaction ($kg_{coke}\ (kg_{cat}\ s)^{-1}$)
$r^{d/a}_{ij}$	integral rate of (dis)appearance of j resulting from reaction i ($mol_{(c)alk}\ (kg_{cat}\ s)^{-1}$)
$\hat{\Re}^o_{c,k}$	calculated average initial coking rate in the experiment k ($kg\ (kg_{cat}\ s)^{-1}$)
$\Re^o_{c,k}$	experimental average initial coking rate for experiment k, ($kg\ (kg_{cat}\ s)^{-1}$)
R_{kj}	net rate of production of a species j in an experiment k ($mol_{(c)alk}\ (kg_{cat}\ s)^{-1}$)
RSS	residual sum of squares $(kg\ (kg_{cat}\ s)^{-1})^2$
TE	tapered element of the TEOM reactor
TEOM	tapered element oscillating microbalance
W	mass of catalyst (kg)
$W/F^o_{c(alk)}$	space-time referred to the inlet molar flow of (cyclo)alkane ($kg_{cat}\ s(mol_{c(alk)})^{-1}$)
y_{kj}	molar yield of species (or lump) j in experiment k

Greek symbols

β-sciss	carbenium ion cracking in beta position
endo-β-sciss	endocyclic cracking in beta position (ring opening)
exo-β-sciss	exocyclic crcking in beta position (dealkylation)
Δm	mass change in the sample bed of the TEOM® reactor (kg)
ϕ	contribution factor
θ^+_B	total fractional catalyst surface concentration of carbenium ions
$\theta^+_{R_1^+}$	fractional catalyst surface concentration with a carbenium ion R_1^+

on the formation of alkanes was observed [9]. The fact that both cracking and coking processes occur in a concerted way implies that they must be simultaneously investigated. The effect of coking on the product distribution can then be explicitly accounted for in the kinetics [10].

Some publications on the kinetic modeling of coke formation [7,11,12] have considered that coke is formed via two steps, viz., a reaction between gas phase coke precursors and adsorbed species leading to a so-called primary coke, and the reaction of the primary coke with gas phase coke precursors to coke growth. From low to moderate coke levels, the occurrence of the second step is not important.

A combination of single-event microkinetic (SEMK) rate equations for the hydrocarbon conversion and global rate equations to account for the effect of coke on the catalyst activity and selectivity has been recently introduced [7]. This paper reports on the application of a SEMK model, which is a fundamental model based on free carbenium ion chemistry, to describe the coking process, based on initial coking rates, during the catalytic cracking of (cyclo)alkanes, viz., *n*-decane, methylcyclohexane and *n*-butylcyclohexane, admixed with 1-octene. So far, the coking process and its effect on the main cracking process have not been modeled simultaneously in terms of single events. Even though temperatures about 50 K below those typically used in the commercial FCC were utilized to filter out the possible influence of thermal reactions, the fundamental nature of the model parameters makes that they are relevant for industrial practice.

2. Experimental and procedures

2.1. Experiments

2.1.1. Set-up

The cracking/coking experiments were performed on a TEOM® microbalance reactor by R&P Co. This is a fixed bed micro-reactor where real time changes in the catalyst mass, for instance due to hydrocarbon adsorption and/or coke deposition, are directly measured non-gravimetrically by the changes induced in the vibration frequency of a tapered element. The

latter, which contains the catalyst bed, is vibrated at constant amplitude at its resonant frequency of oscillation (f). The system determines the mass change of the sample bed between times "0" and "1" as follows:

$$\Delta m = k_0 \left[\frac{1}{f_1^2} - \frac{1}{f_0^2} \right] \quad (1)$$

Δm is the mass change of the catalyst sample, f_0 and f_1 are the natural oscillating frequencies at times "0" and "1", respectively, and k_0 is the spring constant of the tapered element, which is experimentally determined.

In order to determine variations in product distribution with coke deposition and, hence, catalyst mass increase, several samples of the reactor effluent were taken. The first sample was taken at 0.09 ks (1.5 min) to filter out effects caused by pressure imbalances when starting the reaction. Seven additional samples were taken at 0.21, 0.45, 0.78, 1.68, 3.18, 4.80 and 7.1 ks. A typical time on stream amounted to 2 h. The samples at 0.09, 3.18 and 7.1 ks were analyzed on-line, while the others were stored in a ten-way valve and analyzed afterwards. The analysis of the reaction effluent was conducted via chromatography with an FID detector, split inlet and 50 m × 0.20 mm × 0.5 μm PONA capillary. Further details on the experimental set-up have been described elsewhere [13].

2.1.2. Feedstocks

Three (cyclo)alkanes, viz., *n*-decane, methylcyclohexane and *n*-butylcyclohexane, admixed with 1-octene have been investigated. 1-octene has been used to enhance coke formation. The use of relatively simple but representative hydrocarbons allows having a complete characterization via GC analysis of the product spectra. Table 1 shows the range of experimental conditions investigated. A constant inlet molar ratio 1-octene/(cyclo)alkane equal to 0.1765 was maintained. A molar ratio helium/-(cyclo)alkane of 12.0 was set in order to ensure proper vaporization of the hydrocarbons. The partial pressures were varied by adjusting the total pressure in the reactor. The composition of the mixtures was verified via GC analysis to ensure an adequate composition of the gaseous feed before starting the reaction. Blank experiments performed with *n*-decane/1-octene at the maximum temperature, i.e., 753 K, showed the absence of thermal coke and a negligible contribution of thermal cracking in the conversion the (cyclo)alkanes. Care was taken to obtain intrinsic kinetic data, i.e., not affected by transport limitations, for the cracking of the (cyclo)alkanes to focus on the chemical phenomena involved. Plug-flow mode and isobaric reactor operation were also verified.

(Cyclo)alkane conversions ranged from 8 to 70%. The reactivity of these components decreased as follows: *n*-butylcyclohexane >methylcyclohexane> *n*-decane. The cracking of *n*-decane/1-octene led to a mixture of alkanes/alkenes and a small amount of aromatics, while that of methylcyclohexane/1-octene and *n*-butylcyclohexane/1-octene led to alkanes, alkenes, cycloalka(e)nes and aromatics. The coke content evolved from 0.05 to 0.3 wt%. Relatively low coke levels were observed. This can be attributed to the nature of the investigated (cyclo)alkanes and the type of catalyst used together with particular experimental conditions, i.e., relatively low hydrocarbon inlet partial pressures [13]. Since thermal coke was not detected and the metals content on the catalyst is not dramatically high, it is assumed that the observed coke is formed via a catalytic mechanism.

2.1.3. Catalyst

A commercial REUSY (Rare-Earth modified UltraStable Y zeolite) equilibrium catalyst withdrawn from a partial combustion unit was provided by TOTAL. The catalyst has a BET surface area equal to 169 $m^2\,g^{-1}$, a metal content of 1300 ppm V and 670 ppm Ni and a unit cell size of 2.475 nm. In all the experiments, 0.100 g of catalyst was used. After each cracking experiment, the catalyst was regenerated in-situ under 120 ml min^{-1} of air at 813 K for 10 h. Conversions and product distributions could be reproduced after catalyst regeneration.

More details about the experimental procedures, analytical methods, feedstocks and catalyst have been reported elsewhere [13].

2.2. Parameter estimation and reactor model

SEMK have been applied to model coke formation based on initial coking rates. For the estimation of the corresponding kinetic parameters, the following objective function has been minimized:

$$\mathrm{RSS(b)} = \sum_{k=1}^{n_{\mathrm{exp}}} \left(\hat{\Re}^{\mathrm{o}}_{\mathrm{c},k} - \Re^{\mathrm{o}}_{\mathrm{c},k} \right)^2 \xrightarrow{\mathrm{b}} \min \quad (2)$$

The response used in the regression is the average initial coking rate over the catalyst bed. In Eq. (2), $\hat{\Re}^{\mathrm{o}}_{\mathrm{c},k}$ denotes the calculated value and $\Re^{\mathrm{o}}_{\mathrm{c},k}$ the experimentally observed value in experiment k, whereas b is the vector of parameters to be determined and n_{exp} is the number of experiments. ODRPACK

Table 1
Range of experimental conditions during the catalytic cracking of the (cyclo)alkane/1-octene mixtures and corresponding initial coking rates

(Cyclo)alkane	Temperature (K)	$W/F^{\mathrm{o}}_{\mathrm{c(alk)}}$ ($\mathrm{kg_{cat}\ s(mol_{c(alk)})^{-1}}$)	Total pressure (kPa)	Inlet partial pressure (kPa)		Initial coking rate, 10^{-6} $\mathrm{kg_{coke}(kg_{cat}\ s)^{-1}}$
				(Cyclo)alkane	1-Octene	
n-Decane	693–753	12.0–45.7	200–400	13.6–26.6	2.4–4.6	0.24–2.8
Methylcyclohexane	693–753	12.1–42.3	400	26.6	4.6	0.22–0.43
n-Butylcyclohexane	693–753	9.4–34.0	400	26.6	4.6	0.12–0.52

2.01 solver [14] was used to find the parameters that minimize the objective function defined above by nonlinear ordinary least squares for explicit models with an implementation of the Levenberg-Marquardt method.

Experimentally, the coke content of the catalyst is continuously measured and, hence, the average initial experimental coking rate, $\Re_c^o$, can be easily obtained. In contrast, the corresponding calculated average initial coking rates, $\hat{\Re}_c^o$, have to be calculated via integration of the local coking rates along the catalyst bed as follows:

$$\hat{\Re}_c^o = \frac{1}{W}\int_0^W r_c^o \mathrm{d}W \tag{3}$$

The integral of the right-hand side of Eq. (3) is numerically approximated by using the trapezoid formula and, hence, the calculated average initial coking rates are finally given by:

$$\hat{\Re}_c^o = \frac{1}{2n_{step}}[r_{c,1}^o + 2r_{c,2}^o + \ldots + 2r_{c,n_{step}-1}^o + r_{c,n_{step}}^o] \tag{4}$$

In Eq. (4), the differential mass of catalyst, dW, is replaced by ΔW, while the catalyst mass interval was divided in n_{step}, typically 20, elements. $r_{c,i}^o$, the calculated initial coking rate for the catalyst mass in the reactor differential element i, depends on the gas phase composition, i.e., on the partial pressure of the corresponding gas phase coke precursors, and on the concentration of the surface coke precursors, cfr. infra. In the fixed bed reactor, the coking rate varies with the axial position because of changes in the gas phase composition, i.e., coke precursors, along the catalyst bed. The gas phase composition of the different species is obtained via integration of the corresponding reactor model equations given by:

$$\frac{\mathrm{d}y_{kj,\mathrm{calc}}}{\mathrm{d}(W/F_{(c)alk}^o)_k} = R_{kj} \tag{5}$$

$$\text{at}\left(\frac{W}{F_{\left(c\right)alk}^o}\right)_k = 0; \quad y_{kj} = 0$$

The net production rate of a species j in an experiment k, R_{kj} in Eq. (5), is a function of the partial pressure of the involved hydrocarbons and of the rate coefficients for the cracking reactions participating involved in the production or consumption of species j. For computing the latter, reported values of activation energies, estimated via regression, and preexponential factors, calculated a priori via transition state theory and statistical thermodynamics, have been utilized [15]. Notice that the rate coefficients for the cracking reactions are not adjusted during the estimation of the kinetic parameters for the coking model but are used as fixed values. For the same reason, only the details concerning the derivation of the model for coke are given in this work. The set of ODEs represented by Eq. (5) has been derived for a continuous, pseudo-homogeneous and one-dimensional reactor model. The reactor has been operated in the integral regime in the absence of concentration and thermal gradients and has exhibited a plug-flow and an isobaric behavior. The integration of the ODEs has been by using LSODA integration routine discussed in [16].

In this work, coking rates and product yields measured at 0.090 ks were considered as a reasonable approximation for initial conditions rather than extrapolated values to time zero because such extrapolations may lead to erroneous results due to the corresponding profiles.

2.3. Contribution analysis

A contribution analysis of the reaction families involved in the coking model was performed based on the methodology described by Chen et al. [17]. This methodology is based on reaction rates and, hence, accounts for the effects of rate coefficients and of reactant concentration.

In general, the integral (dis)appearance (d/a) contribution factor (ϕ) of the elementary step i toward the (dis)appearance of component j for a given experiment k is defined as the ratio of the rate of (dis)appearance of j resulting from reaction i, $r_{ij}^{\mathrm{d/a}}$, to the total rate of (dis)appearance of j at a certain position inside the reactor:

$$\phi_{ij}^{\mathrm{d/a}} = \frac{r_{ij}^{\mathrm{d/a}}}{\sum_i r_{ij}^{\mathrm{d/a}}} \tag{6}$$

Integral contribution factors are determined by using the rates integrated over the reactor position.

3. SEMK model for coking based on initial coking rates

SEMK accounts for the detailed carbenium ion chemistry occurring on the Brønsted acid sites of zeolitic catalysts. It uses rate coefficients which are estimated through the cracking of relatively simple but well chosen model molecules [18] and can be applied to any feedstock.

A SEMK model to describe coke formation during the catalytic cracking of hydrocarbons has been recently developed [10]. It is being applied in the current work to model coke formation during the cracking of the three investigated mixtures of (cyclo)alkane/1-octene. Coke is proposed to be formed out of gas phase and surface coke precursors. The formation of these coke precursors together with their transformation to coke is entirely described in terms of the same families of elementary steps, i.e., hydride transfers, alkylations, cyclisations and deprotonations, as those involved in the cracking process. Moreover, the formation of the coke precursors is strictly reversible whereas the critical step for the transformation of the coke precursors to coke is proposed to occur through irreversible alkylations. In principle, all species susceptible to alkylation are potential coke precursors, in practice a species was considered as coke precursor when the corresponding alkylated product was rather bulky, cfr. infra.

3.1. Reaction pathways and rate-determining steps to coke

The application of the SEMK for coking starts with the identification of possible reaction pathways and the participating

species, i.e., gas phase and surface coke precursors, along with the definition of the rate-determining steps to coke. Experimental findings and information reported in the literature, vide introduction, have been utilized in the formulation of the kinetic model.

A qualitative analysis of the experimental cracking/coking has been reported in our previous work [13]. Such an analysis has been of great utility to devise a set of possible reaction pathways. The differences in coke formation observed during the cracking of the (cyclo)alkane/1-octene mixtures indicate that not only the 1-octene, added to enhance the amount of coke, but also the products formed out of the (cyclo)alkanes are involved in the coking processes.

Fig. 1, for instance, illustrates the behaviour of the initial coking rates for *n*-decane/1-octene and *n*-butylcyclohexane/1-octene as a function of the initial (cyclo)alkane conversion in the temperature range 693–753 K for a given hydrocarbon partial pressure. The increase of the initial coking rate with the (cyclo)alkane conversion demonstrates the involvement of the cracked products out of the (cyclo)alkanes in coking. From

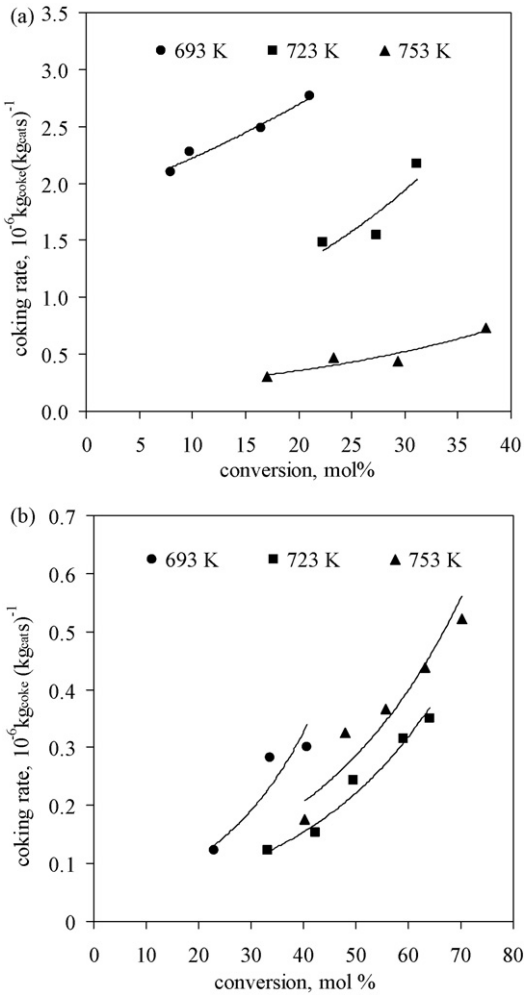

Fig. 1. Initial experimental coking rate vs. molar (cyclo)alkane conversion for the catalytic cracking of the hydrocarbon mixtures at 693–753 K, $P^{o}_{p\,(c)alk}$ = 26.6 kPa, $P^{o}_{p\,1\text{-octene}}$ = 4.8 kPa, space-time = 9.4–45.7 kg_{cat} s $(mol_{(c)alk})^{-1}$. (a) *n*-decane/1-octene and (b) *n*-butylcyclohexane/1-octene. Full lines are used only for showing trends.

Fig. 1 it is also clear that, for a given (cyclo)alkane conversion, there are differences in the coking rates for the different (cyclo)alkane/1-octene mixtures, e.g., *n*-decane/1-octene displays higher coking rates compared with *n*-butylcyclohexane/1-octene. The values of the initial coking rates from methylcyclohexane/1-octene are rather similar to those observed from *n*-butylcyclohexane/1-octene as can be inferred from Table 1. Initial coking rates out of pure *n*-octene are higher than the coking rates observed when feeding a (cyclo)alkane/1-octene mixture. The higher the reactivity of the (cyclo)alkane in the mixture, the more the initial coking rate decreased.

Due to the relatively simple structure of the investigated (cyclo)alkanes, heavy hydrocarbons, e.g., polyaromatics, were not detected in the reactor effluent. As a result, other aromatics more abundantly observed in the reactor effluent have been proposed as gas phase coke precursors. Monoaromatics, which were observed in relatively high amounts during the cracking of the (cyclo)alkane/1-octene feeds [15], in particular out of cycloalkanes, can also react via alkylation in an analogous way as was proposed for polyaromatics [10] for producing coke. This assumption is reasonable by considering that the structure of the resulting coke is determined by the complexity of the feedstock and, hence, the complexity of the coke precursors is also expected to vary.

Due to the inherent complexity that accompanies the coking process, it has been convenient to define rate-determining steps for coke formation. Two rate-determining steps for coke formation involving aromatics have been proposed:

i. alkylation of phenyl substituted carbenium ions with C_3–C_5 alkenes.
ii. alkylation of the nucleus of monoaromatics with C_3–C_5 alkylcarbenium ions.

A third rate-determining step to describe coke involving alkylation of acyclic species basically associated to 1-octene has also been proposed:

iii. alkylation of C_8–C_{10} alkylcarbenium ions with C_3–C_5 alkenes.

A schematic representation of the proposed rate-determining steps is shown in Table 2. The alkylation reactions used to describe coke formation are considered as irreversible steps. The alkenes which act as alkylating agents are typically present in relatively high amounts in the gas phase because these are not susceptible to further cracking. This choice leads to an adequate description of the experimental initial coking rates, cfr. infra.

In the following paragraphs, the reaction pathways involved in the coking during the cracking of pure 1-octene and the three (cyclo)alkanes in the presence of 1-octene are described. The rate-determining steps to coke are further discussed.

3.1.1. Coking reaction pathway starting from 1-octene

In Fig. 2, the coking pathways during the 1-octene conversion are drawn. The conversion of 1-octene starts with a protonation leading to a large concentration of *n*-octyl carbenium ions on the catalyst surface. These carbenium ions undergo skeletal isomerization to produce more stable mono, di

Table 2
Summary of the postulated rate-determining steps to coke during the cracking of the (cyclo)alkane/1-octene mixtures

	coke precursors			Rate-determining step			
	Gas phase		Surface				
(i)	O_j	+	A_k^+	$\xrightarrow{\text{side chain alk}}$			
(ii)	A_i	+	C_j^+	$\xrightarrow{\text{nucl alk}}$	"Alkylated coke precursors"	$\longrightarrow_{\text{fast}}$	Coke
(iii)	O_j	+	C_k^+	$\xrightarrow{\text{alk}}$			

With j = 3–5; i = 6–10; k = 8–10.

and trimethyl branched alkylcarbenium ions which are, however, susceptible to β-scission. Experimentally, it was found that the cracking of 1-octene yields a significant amount of alkenes in the range C_3–C_5 [15]. Since protonation of alkenes is an easy reaction [19], (branched) carbenium ions out of 1-octene, denoted as C_8^+, moC_8^+, diC_8^+, etc., in Fig. 2, are readily available for other consecutive reactions. With a lot of C_3–C_5 alkenes being produced, the (branched) carbenium ions out of 1-octene are likely to undergo alkylation with these gas phase C_3–C_5 alkenes. The latter reaction corresponds to the rate-determining step to coke denoted as (iii). This alkylation results in oligomers that are assumed to be converted very rapidly to coke. Oligomers formed during the cracking of alkenes have been identified as responsible for coke formation. They are bulky species, i.e., typically dibranched species with a propyl-, (iso)butyl- or (iso)pentyl-branch and a minimum carbon number of 11, that can eventually remain adsorbed in the catalyst pores [20].

1-Octene is also involved in coke formation through aromatics, the latter being the gas phase coke precursors as is also shown in Fig. 2. This pathway starts with the formation of alkenylcarbenium ions out of 1-octene via hydride transfer. When the positive charge of the alkenylcarbenium ion is in delta or gamma position, cyclisation can occur yielding a cycloalkylcarbenium ion, N_8^+. When the latter carbenium ion has a cyclohexyl structure, it can be converted to aromatics, through a sequence of deprotonation/hydride transfer steps. Even though the protonation of 1-octene is expected to be favored over the hydride transfer of the saturated part of 1-octene to form alkenylcarbenium ions, the occurrence of the latter reaction pathway is experimentally demonstrated by the presence of xylenes in the reactor effluent when cracking 1-octene [15]. Xylenes formed this way are assumed to be alkylated via an electrophylic attack by carbenium ions, cfr. rate-determining step to coke (ii), to produce an alkylated aromatic, which is also assumed to transform to coke very rapidly in a similar manner as described for the oligomers above. The alkylated aromatics species have a carbon number of at least 11 and have more than one side chain. At least one of these side chains is a propyl-, (iso)butyl- or (iso)pentyl-group.

3.1.2. Coking reaction pathway starting from (cyclo)alkanes in the presence of 1-octene

The differences in coking experimentally observed during the cracking of the (cyclo)alkane/1-octene mixtures indicate that (cyclo)alkane cracked products participate in the coking processes with products associated to 1-octene.

For *n-decane*, coke formation is proposed to occur in an analogous way as for 1-octene. C_{10}-carbenium ions formed out of *n*-decane via hydride transfer may contribute to coke formation via alkylation with small alkenes, rate-determining step to coke (iii). In addition, despite their low gas phase concentration, aromatics formed from *n*-decane via cyclisation and deprotonation/hydride transfer steps, have been also accounted for in coking. The corresponding aromatic carbenium ions can be alkylated on the side chain, rate-determining

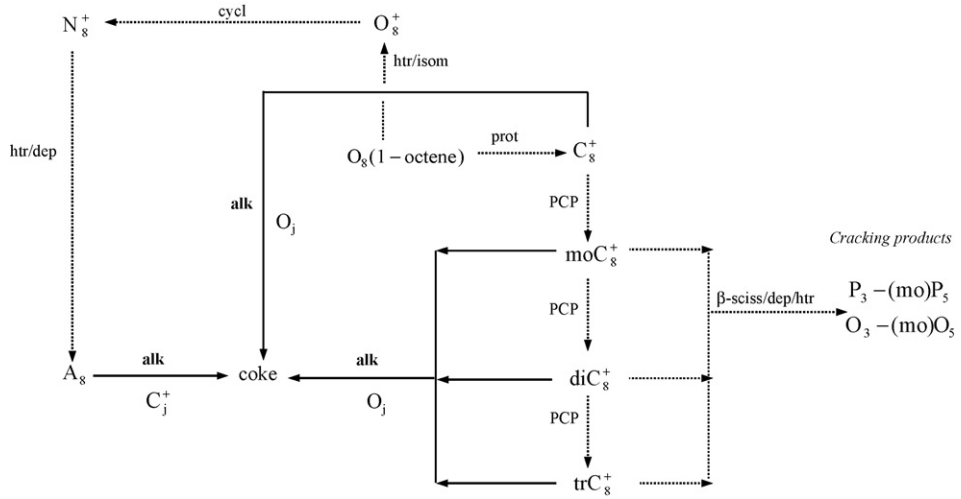

Fig. 2. Reaction pathways involved in the coking of 1-octene at the carbenium ion level. P, O, C^+ and O^+ are for alkanes, alkenes, alkylcarbenium ions and alkenylcarbenium ions. Mo, di and tr are for methyl, dimethyl and trimethyl substituted species. Dashed arrows are used for the steps not strictly involved in coking.

step to coke (i), or the aromatics can be alkylated at the nucleus, rate-determining step to coke (ii).

Concerning the possible routes to coke formation departing from *methylcyclohexane*, cycloalkylcarbenium ions formed out of methylcyclohexane via hydride transfer are transformed to aromatics through a series of hydride transfer/deprotonation steps. Both toluene and xylenes react with adsorbed alkylcarbenium ions via nucleus alkylation according to rate-determining step to coke (ii). Side chain alkylation, i.e., rate-determining step to coke (i), could also occur on ethylbenzene (or higher alkylbenzenes) when the corresponding carbenium ions formed via hydride transfer are alkylated with small gas phase alkenes. The resulting alkylated species formed via nucleus or side chain alkylation can be considered as coke.

The reaction pathways for coke formation out of *n-butylcyclohexane* appear to be more complex than those described out of methylcyclohexane, because of the presence of heavier aromatics, as depicted in Fig. 3. Because the number of reaction possibilities for *n*-butylcyclohexane is drastically higher than for methylcyclohexane, side chain alkylation of aromatic carbenium ions with light alkenes, rate-determining step to coke (i), is expected to have an increasingly important contribution to coke formation. Aromatics in the gas phase are produced ''directly'' from *n*-butylcyclohexane via hydride transfer and deprotonation steps, or from cyclic hydrocarbons formed via exocyclic β-scission, also followed by hydride transfer and deprotonation. The formed alkylated species will also have at least 11 carbon atoms with at least one side chain having 5 carbon atoms. Diaromatics formation is also possible, however, the amount of diaromatics present in the reaction effluent was low compared to that of other potential coke precursors.

3.2. Model construction

3.2.1. Reaction types and rate coefficients

According to the different rate-determining steps in the reaction pathway to coke and considering the nature of the involved carbenium ions, i.e., secondary or tertiary, ten reaction types and corresponding rate coefficients strictly associated to coke can be defined. Two alkylations of the nucleus of aromatics with C_3–C_5 alkylcarbenium ions, four alkylations of C_8–C_{10} alkylcarbenium ions with C_3–C_5 alkenes and four alkylations of the chain of aromatic carbenium ions with the same alkenes. Defining a rate coefficient per reaction type and, hence, one activation energy and preexponential factor, values for 20 kinetic parameters are to be obtained.

A first reduction in the number of parameters is possible by considering that the side chain alkylation of aromatic carbenium ions is analogous to the alkylation of acyclic alkylcarbenium ions. As a result, only four rate coefficients are sufficient to describe (side chain) alkylation, decreasing the number of reaction types involved in coke formation from 10 to 6 and the number of kinetic parameters from 20 to 12. This number can be further reduced by assuming that the structure of the alkylated species in (side chain) alkylation does not have any effect on the coking reaction rates as they are being considered as coke. Hence, two rate coefficients that only depend on the nature of the reactant carbenium ion, i.e., secondary or tertiary, are sufficient to describe (side chain)

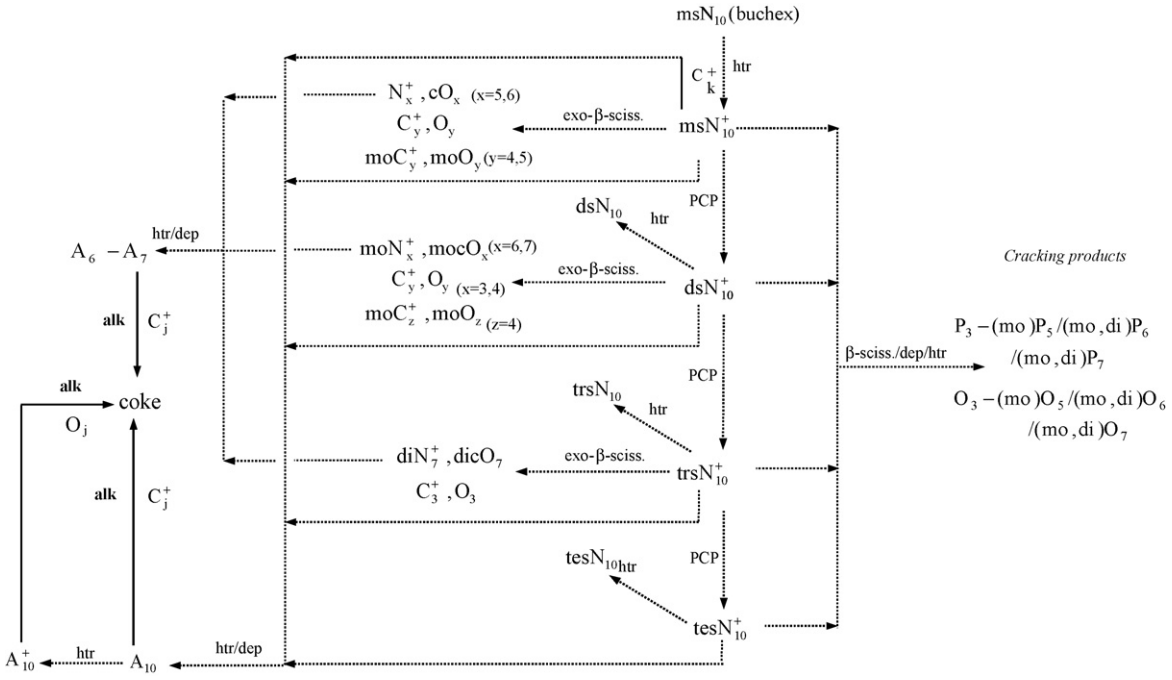

Fig. 3. Reaction pathways involved in the coking of *n*-butylcyclohexane in the presence of 1-octene at the carbenium ion level. P, O, C^+, O^+, N^+, A, A^+, and cO and are for alkanes, alkenes, alkylcarbenium ions, alkenylcarbenium ions, cycloalkylcarbenium ions, aromatics, aromatic carbenium ions and cycloalkenes. Ms, ds, trs and tes are for mono, di, tri and tetra substituted cycloalkanes or cyclic carbenium ions. Mo, di and tr are for methyl, dimethyl and trimethyl substituted species. Dashed arrows are used for the steps not strictly involved in coking.

Table 3
Summary of the reaction possibilities for the (side chain) alkylations and the nucleus alkylations involved in coke formation according to the existing network

Alkylation type	Number of reaction types				
	(s, s)	(s, t)	(t, s)	(t, t)	Total
Non-branched C_8 alkylcarbenium ions	12	6	0	0	18
Branched C_8 alkylcarbenium ions	76	16	28	4	124
Side chain alkylation of aromatic carbenium ions	100	36	45	7	188
	(s)		(t)		Total
Nucleus alkylation of aromatics	1298		274		1572

alkylation. These rate coefficients are denoted as:

$$(\text{side\_chain})\ \text{alkylation}: \tilde{k}_{\text{alk\_side}}(\text{s}),\ \tilde{k}_{\text{alk\_side}}(\text{t})$$

For the nucleus alkylation of aromatics that occurs via electrophylic attack by an alkylcarbenium ion, two reaction types (rate coefficients) are involved depending on the nature of the latter:

$$\text{nucleus alkylation}: \quad \tilde{k}_{\text{alk\_nucl}}(\text{s}),\ \tilde{k}_{\text{alk\_nucl}}(\text{t})$$

This way, the final number of kinetic parameters to be obtained via regression amounts to 8. This number can be further reduced to 4 by calculating the corresponding preexponential factors via transition state and statistical thermodynamics concepts, cfr. infra. Table 3 shows a summary of the alkylations considered as the rate-determining steps in coking at the molecular level.

3.2.2. Relumped SEMK rate equations

The SEMK model in the so-called relumped form has been applied to describe the initial coke formation out of the (cyclo)alkane/1-octene mixtures investigated. For hydrocarbons with small carbon numbers, SEMK simulations can be performed at the molecular level, however, for hydrocarbons with higher carbon numbers the reaction network becomes so overwhelming that the solution of the corresponding set of equations becomes practically impossible [21,22]. In addition, an analysis in full detail of the reaction products for such carbon numbers is impossible with today's analytical tools. Note that this relumping preserves the fundamental character of the model.

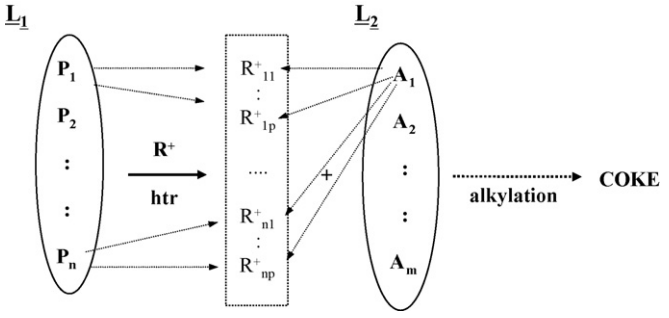

Fig. 4. Lumped scheme for the transformation of alkenes in lump L_1 and aromatics in lump L_2 to coke via nucleus alkylation of the latter hydrocarbons. R^+ are carbenium ions formed via hydride transfer of alkanes in lump L_1.

An example of the construction of the relumped SEMK rate equations for the nucleus alkylation of aromatics involved in coking is given. For instance, a lump L_2 composed by aromatic hydrocarbons reacts with alkylcarbenium ions that are formed out of alkanes contained in lump L_1, as is schematically represented in Fig. 4. Here, the alkylcarbenium ions are formed from lump L_1 via hydride transfer, while aromatics in lump L_2 undergo alkylation on the nucleus with these carbenium ions. At the molecular level, the rate equation for the transformation of all the carbenium ions formed out of L_1 with the aromatics in lump L_2 to coke via nucleus alkylation is expressed by:

$$\begin{aligned}(r_{\text{c}}^{\text{o}})_{\text{alk\_nucl}}(\text{L}_1+\text{L}_2\rightarrow\text{coke}) &= \sum_s n_{\text{e}}\tilde{k}_{\text{alk\_nucl}}(\text{s})\theta^+_{\text{R}_1}(\text{s})P_{\text{A}_j}\text{Mw}_{\text{coke}} \\ &+ \sum_t n_{\text{e}}\tilde{k}_{\text{alk\_nucl}}(t)\theta^+_{\text{R}_1}(\text{t})P_{\text{A}_j}\text{Mw}_{\text{coke}}\end{aligned} \tag{7}$$

Notice that all the possible transformations, i.e., those involving secondary and tertiary carbenium ions, are taken into account.

By including the so-called relumping coefficients, Eq. (7) can be rewritten as:

$$\begin{aligned}(r_{\text{c}}^{\text{o}})_{\text{alk\_nucl}}(\text{L}_1+\text{L}_2\rightarrow\text{coke}) &= \tilde{k}_{\text{alk\_nucl}}(\text{s})\text{Mw}_{\text{coke}}\text{LC}_{\text{alk\_nucl}}(\text{s})\theta_{\text{R}_1^+}(\text{s})P_{\text{L}_2} \\ &+ \tilde{k}_{\text{alk\_nucl}}(\text{t})\text{Mw}_{\text{coke}}\text{LC}_{\text{alk\_nucl}}(\text{t})\theta_{\text{R}_1^+}(\text{t})P_{\text{L}_2}\end{aligned} \tag{8}$$

whereby P_{L_2} is the partial pressure of lump L_2, the gas phase coke precursor. $\tilde{k}_{\text{alk\_nucl}}$ is the single-event rate coefficient for the nucleus alkylation. Mw_{coke} can be taken as the sum of the molecular mass of the gas phase and the surface coke precursors in the case of initial coking [23]. $\theta_{\text{R}_1^+}(\text{s})$ and $\theta_{\text{R}_1^+}(\text{t})$ correspond to fractional catalyst surface concentration of secondary and tertiary carbenium ions formed out of lump L_1 via hydride transfer and can be obtained by applying the pseudo steady-state approximation for the formation/consumption of carbenium ions from lump L_1. For tertiary carbenium ions this leads to:

$$\theta_{\text{R}_1^+}(\text{t}) = \frac{\theta^+_{\text{B}}\tilde{k}_{\text{htr}}(\text{t})P_{\text{L}_1}}{(n_{\text{e}})_{\text{dep,av}}\tilde{k}_{\text{dep}}(\text{t}) + \tilde{k}_{\text{htr}}(\text{s})\sum_j (n_{\text{e}})_{\text{htr}}P_{\text{L}_j} + \tilde{k}_{\text{htr}}(\text{t})\sum_j (n_{\text{e}})_{\text{htr}}P_{\text{L}_j}} \tag{9}$$

The numerator of Eq. (9) corresponds to the rate of appearance of carbenium ions via hydride transfer out of L_1, whereas the denominator accounts for the rate of disappearance of the same carbenium ions via deprotonation and hydride transfer. θ_B^+ is the total fractional catalyst surface concentration of carbenium ions that can participate in hydride transfer. $\tilde{k}_{dep}$, $\tilde{k}_{prot}$ and $\tilde{k}_{htr}$ are the deprotonation, protonation and hydride transfer single-event rate coefficients for the cracking reactions determined in the absence of coke formation [15]. P_{L_1} is the partial pressure of lump L_1.

In Eq. (8), LC_{alk_nucl}, the lumping coefficient corresponding to alkylation, depends on the reaction network and on the lumps definition and is determined by:

$$LC_{alk\_nucl}(m) = \sum_m (n_e)_{alk\_nucl}(n_e)_{htr}\, y_{i,L_1} y_{j,L_2} \quad (10)$$

$(n_e)_{alk\_nucl}$ and $(n_e)_{htr}$ is the number of single events for side chain alkylation and hydride transfer, while y_{i,L_1} represents the molar fraction of the alkane i in the lump L_1 and y_{j,L_2} the molar fraction of the aromatic j in the lump L_2.

After incorporating coke formation in the relumped SEMK model, the latter consists of 107 lumps. 106 lumps for the gas phase hydrocarbons in the range C_1–C_{12}, viz., 35 of alkanes, 34 of alkenes, 10 of cycloalkanes, 10 of cycloalkenes, 10 of cycloalkadienes and 7 of aromatics, and one independent lump for coke. Values for the rate coefficients corresponding to the reaction types discussed in Section 3.2.1. have been obtained from separate regressions for the various (cyclo)alkane/1-octene mixtures.

3.2.3. Parameter values

A non-isothermal regression utilizing the available experimental coking data was performed to estimate the activation energies for the reaction types involved in the coking model. Hence, the Arrhenius equation in reparameterized form was required:

$$\tilde{k} = A_{rep}\exp\left[-\frac{E}{R}\left(\frac{1}{T}-\frac{1}{T_m}\right)\right] \quad (11)$$

$$A_{rep} = C_{t,H^+}\tilde{A}\exp\left[-\frac{E}{RT_m}\right] \quad (12)$$

$\tilde{k}$ is the single-event rate coefficient while E and A_{rep} are the activation energy and reparameterized preexponential factor for a given elementary reaction. T_m is the average temperature over the experiments and $\tilde{A}$ the single-event preexponential factor. In order to reduce the number of kinetic parameters to be handled simultaneously, preexponential factors, were not estimated but calculated a priori via transition state theory and statistical thermodynamics [24–26]. A preexponential factor equal to 1.9×10^7 (kPa s)$^{-1}$ was obtained for the alkylations considered as rate-determining steps for coke, by assuming that the transition state species has lost two translational degrees of freedom compared to the reactant state. This value is thermodynamically consistent with the value obtained by Martens et al. [26] for β-scission.

In Eq. (10) C_{t,H^+}, the total concentration of acid sites on the catalyst is fixed at the value already estimated via regression for the cracking reactions [15]. The latter amounts to 0.157 mol $(kg_{cat})^{-1}$.

The calculated average initial coking rate that is calculated via Eq. (4) depends on the gas phase composition and on the rate coefficients for the reaction families involved in the cracking reactions. The gas phase composition according to Eq. (5) is a function of the corresponding net production rate that also depends on the rate coefficients for the cracking reactions. The rate coefficients for the latter were estimated by using the experimental data of the cracking of the same (cyclo)alkane/1-octene mixtures in the absence of coke formation as has been reported in [15]. Recall that these rate coefficients were kept constant during the estimation procedure of the activation energies for the coking reactions, cfr. Section 2.2.

The activation energies for the coking model were estimated for each one of the (cyclo)alkene/1-octene feeds, using 15, 14 and 13 experiments for *n*-decane/1-octene, methylcyclohexane/1-octene and *n*-butylcyclohexane/1-octene, respectively. The corresponding degrees of freedom are 13, 12 and 11, which are rather low due to the low number of experiments.

Table 4 displays the values of the estimated activation energies as well as some statistical information obtained via regression of the different hydrocarbon mixtures coking data. For both nucleus alkylation and (side chain) alkylation, it was impossible to estimate significantly the two rate parameters associated to each alkylation because they were strongly correlated. It is clear that, taken into consideration the obtained confidence intervals, the obtained activation energies for the secondary (side chain) alkylation mode and for the nucleus alkylation (from cycloalkane/1-octene mixtures) proceeding via secondary carbenium ions obtained are independent of the

Table 4
Activation energies and corresponding confidence intervals at 95% probability level for the alkylation reactions involved in coke formation during the catalytic cracking of the various (cyclo)alkane/1-octene mixtures

Data used in the regression	E_{act} (kJ (mol)$^{-1}$)				F_{reg}
	alk(s)	alk(t)	alk_nucl(s)	alk_nucl(t)	
n-Decane/1-octene	–	135.6 ± 5.4	–	97.5 ± 7.3	58.5
Methylcyclohexane/1-octene	101.5 ± 3.4	–	115.7 ± 1.2	–	60.3
n-Butylcyclohexane/1-octene	103.5 ± 3.0	–	122.6 ± 1.3	–	54.0
Methylcyclohexane/1-octene + *n*-butylcyclohexane/1-octene	99.5 ± 2.3	–	121.1 ± 2.6	–	18.9

F_{tab} = 2.91 for 10 degrees of freedom at 95% probability level.

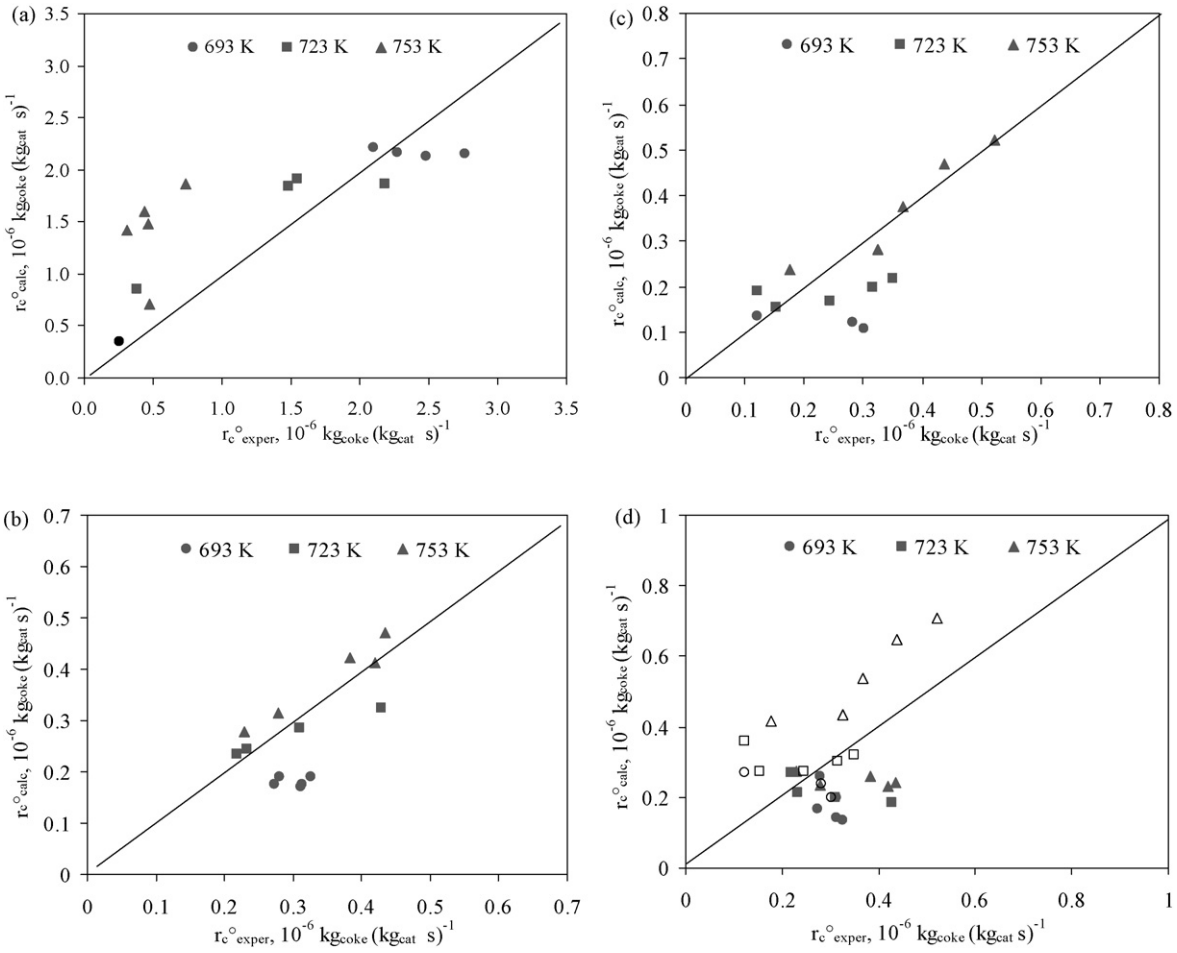

Fig. 5. Parity plots showing simulated vs. experimental initial coking rates for various data regressions over the range of operating conditions displayed in Table 1: (a) *n*-decane/1-octene; (b) methylcyclohexane/1-octene; (c) *n*-butylcyclohexane/1-octene; and (d) simultaneous regression of methylcyclohexane/1-octene (full symbols) and *n*-butylcyclohexane/1-octene (void symbols) data. The coking rates have been computed using Eq. (8) for nucleus alkylation and similar for (side chain) alkylation with a preexponential factor equal to 1.9×10^7 $(kPa\ s)^{-1}$ and activation energies as displayed in Table 4.

feedstock. This reflects the fundamental character of the SEMK model. Although the estimated parameter values are rather close to each other and the 95% confidence intervals (almost) overlap each other, a simultaneous regression using all the data with the three (cyclo)alkanes/1-octene mixtures was not giving satisfactory results. Some effect of the feedstock nature on the rate parameters seems to be left, because a simultaneous regression of only the methylcyclohexane/1-octene and *n*-butylcyclohexane/1-octene data was found to give reasonable results, vide Table 4. A further assessment of these effects falls, however, beyond the scope of the current work.

Moreover (side chain) alkylation reactions involving secondary carbenium ions are energetically favored by about 14–20 kJ mol^{-1} compared with nucleus alkylation showing that the attack on an aromatic ring is more difficult than on a double bond of an alkene. The fact that for nucleus alkylation, the activation energy for the secondary mode was significant for the regression utilizing the cycloalkane/1-octene data and the tertiary mode was for the regression using the *n*-decane/1-octene data, should be explained in terms of a high participation of isopentyl carbenium ions, which are relatively easily formed

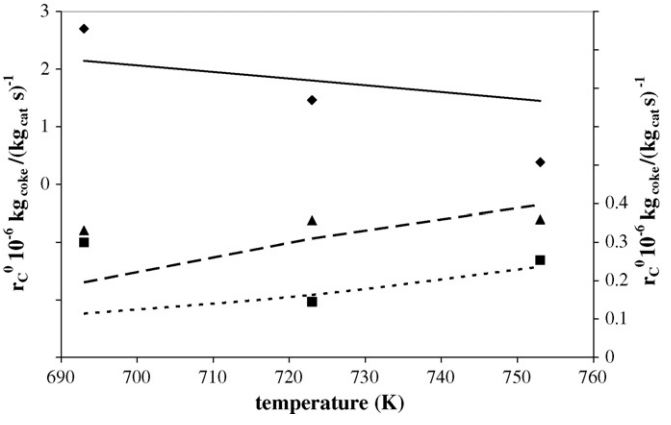

Fig. 6. Initial coking rates as a function of the temperature at a typical conversion, i.e., *n*-decane/1-octene 20%, methylcyclohexane/1-octene 35%, butylcyclohexane/1-octene 40%. Symbols: experimental/lines: calculated; *n*-decane/1-octene (◆)/full line; methylcyclohexane/1-octene (▲)/long-dashed line; butylcyclohexane/1-octene (■)/short-dashed line. The coking rates have been computed using Eq. (8) for nucleus alkylation and similar for (side chain) alkylation with a preexponential factor equal to 1.9×10^7 $(kPa\ s)^{-1}$ and activation energies as displayed in Table 4.

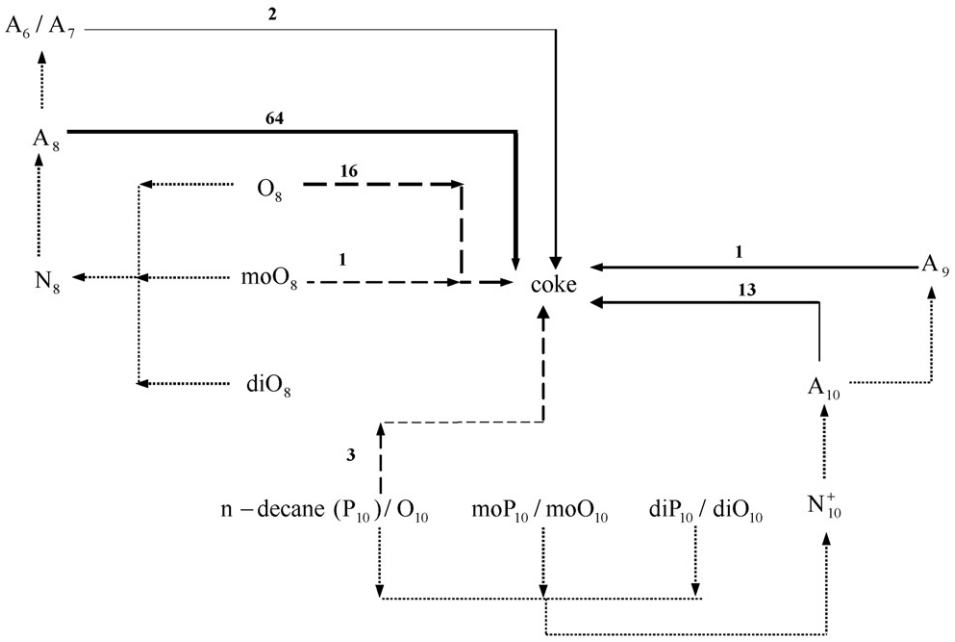

Fig. 7. Contribution analysis for relumped SEMK for coke formation based on initial coking rates out of *n*-decane/1-octene at 723 K, space-time = 26.6 - $kg_{cat}\ s(mol)^{-1}$, $P^{o}_{p\,n-decane}$ = 26.6 kPa, $P^{o}_{p\,1-octene}$ = 4.8 kPa. The coking rates have been computed using Eq. (8) for nucleus alkylation and similar for (side chain) alkylation with a preexponential factor equal to 1.9×10^{7} $(kPa\ s)^{-1}$ and activation energies as displayed in Table 4. For the coking reactions, the numbers at the arrows indicate the procentual contribution of this reaction to coke formation, while the thickness of the arrows is proportional to the rates in logarithmic scale. The contribution of the side chain alkylation of aromatics to coke is negligible. (·····) Reactions not involved in coking; (– – –) coking via alkylation of acyclics; (—) coking via nucleus alkylation of aromatics.

out of the cracking of *n*-decane, in the coking process of the latter mixture.

Parity diagrams, comparing calculated versus experimental initial coking rates, are presented in Fig. 5. They illustrate reasonable model predictions, in particular for methylcyclohexane/1-octene and *n*-butylcyclohexane/1-octene. The highest *F*-value for the significance of the regression has been obtained for the former mixture, vide Table 4. In general, the model is able to simulate the peculiar temperature effects on the coking rates, vide Fig. 6. The decreasing trend of the initial coking rate with the reaction temperature at 20% conversion for *n*-decane/1-octene cracking is represented by the model albeit somewhat less pronounced. Such a decrease in the initial coking rate has also been observed by other authors [8,23,27] and can be explained in terms of an overcompensation of the increase in the alkylation rate coefficients for the rate-determining steps by a decrease in the concentration of surface coke precursors. For methylcyclohexane/1-octene cracking slightly increasing initial coking rates were observed at 35% conversion with increasing temperature while a somewhat more important increase was calculated. The initial coking rates in butylcyclohexane/1-octene cracking at 40% conversion decrease in the range from 693 to 723 K, while an increase is observed from 723 to 753 K. Based on the simulated initial coking rates for butylcyclohexane/1-octene cracking represented in Fig. 6, a minimum initial coking rate is expected at a somewhat lower temperature than observed experimentally. However, in general, Fig. 6 illustrates the model's flexibility in qualitatively describing the diverse trends in observed initial coking rates as a function of the reaction temperature for various feedstocks.

3.3. Contribution analysis

A contribution analysis based on integral contribution factors was performed in order to assess the relative importance of the different reaction families and gas phase coke precursors in coking at specific operating conditions. Due to the different nature of the gas phase coke precursors considered in the model, viz., alkenes and aromatics, it is expected that the relative contribution of reactions and coke precursors depends on the gas phase composition and, hence, the feedstock as well as on temperature and on space-time. In general, preliminary simulations indicate that as temperature and space-time increase, the participation of aromatics in coking becomes more pronounced, independently of the (cyclo)alkane/1-octene mixture.

The results of the contribution analysis for the three (cyclo)alkane/1-octene mixtures at 723 K and at identical inlet conditions utilizing the kinetic parameters in Table 4 are presented in Figs. 7–9. In these figures, the numbers next to the arrows indicate the relative contribution to coke for the different gas phase coke precursors and corresponding coking reactions. The thickness of the arrow indicates the relative magnitude of the coking rate in the logarithmic scale. Notice that the use of a relumped model means that the conversion of the various lumps to coke involves more than one elementary step. For instance, the alkylation of C_8-alkenes with small alkenes requires a preliminary protonation of the former hydrocarbons to occur.

Out of *n-decane/1-octene*, the amount of coke formed via side chain alkylation of aromatics with small alkenes was found

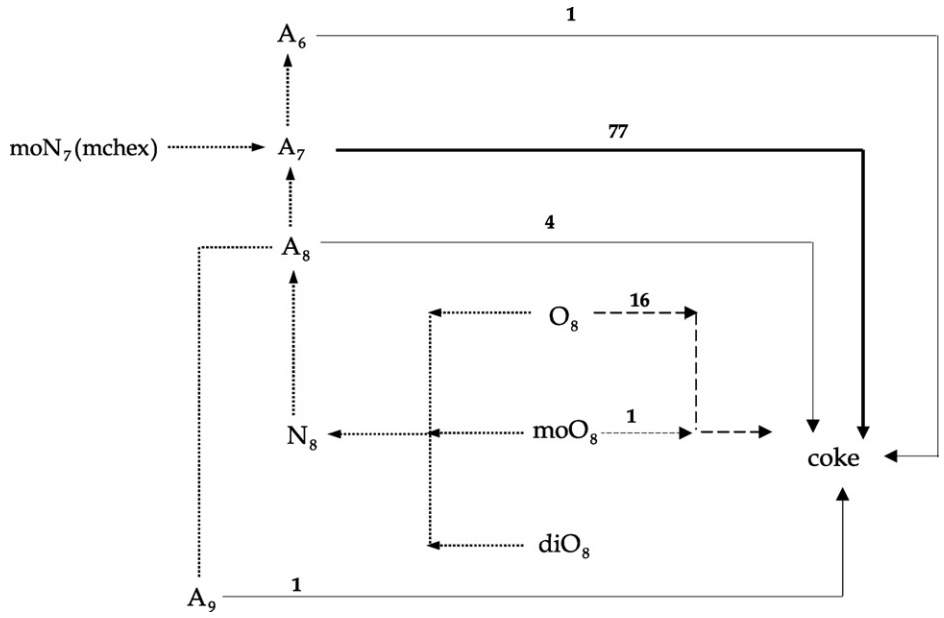

Fig. 8. Contribution analysis for relumped SEMK for coke formation based on initial coking rates out of methylcyclohexane/1-octene at 723 K, space-time = 26.6 kg_{cat} s(mol)$^{-1}$ and $P^{o}_{p\,mchex}$ = 26.6 kPa, $P^{o}_{p\,1-octene}$ = 4.8 kPa. The coking rates have been computed using Eq. (8) for nucleus alkylation and similar for (side chain) alkylation with a preexponential factor equal to 1.9×10^{7} (kPa s)$^{-1}$ and activation energies as displayed in Table 4. For the coking reactions, the numbers at the arrows indicate the procentual contribution of this reaction to coke formation, while the thickness of the arrows is proportional to the rates in logarithmic scale. The contribution of the side chain alkylation of aromatics to coke is negligible. (·····) Reactions not involved in coking; (– – –) coking via alkylation of acyclics; (—) coking via nucleus alkylation of aromatics.

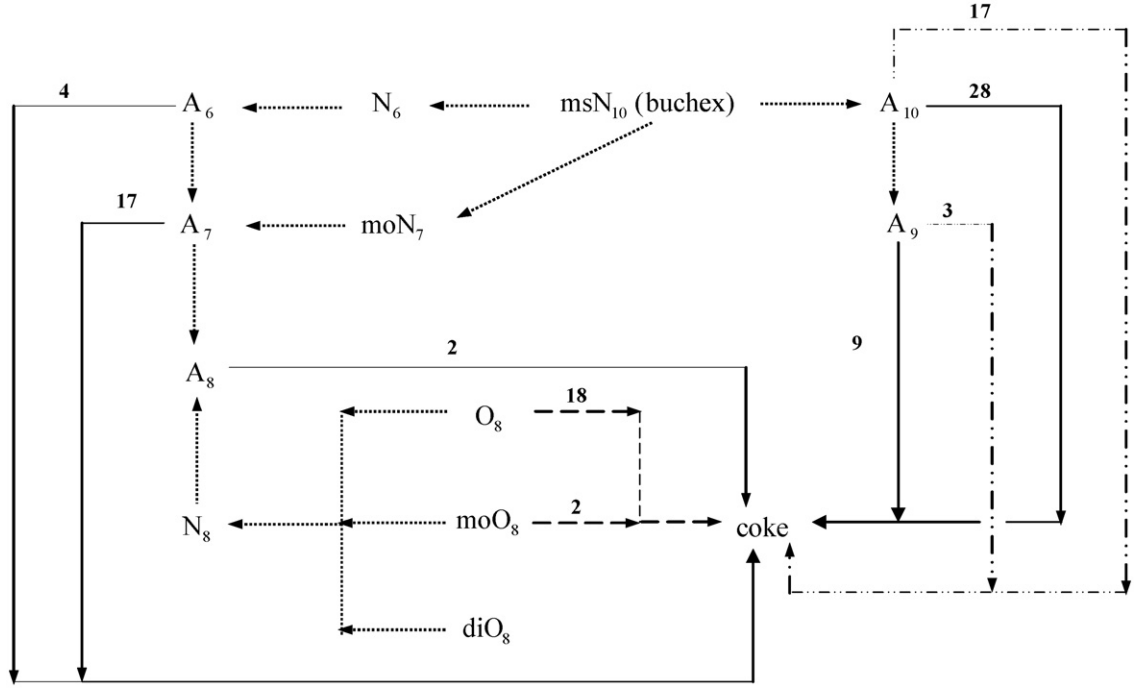

Fig. 9. Contribution analysis for relumped SEMK for coke formation based on initial coking rates out of *n*-butylcyclohexane/1-octene at 723 K, space-time = 26.6 kg_{cat} s(mol)$^{-1}$ $P\mathrm{p}^{o}_{n-buchex}$ = 26.6 kPa, $P\mathrm{p}^{o}_{1-octene}$ = 4.8 kPa. The coking rates have been computed using Eq. (8) for nucleus alkylation and similar for (side chain) alkylation with a preexponential factor equal to 1.9×10^{7} (kPa s)$^{-1}$ and activation energies as displayed in Table 4. For the coking reactions, the numbers at the arrows indicate the procentual contribution of this reaction to coke formation, while the thickness of the arrows is proportional to the rates in logarithmic scale. (·····) Reactions not involved in coking; (– – –) coking via alkylation of acyclics; (—) coking via nucleus alkylation of aromatics; (·—·—) coking via side alkylation of aromatics.

to be negligible. According to Fig. 7, the nucleus alkylation of aromatics, in particular A_8, and A_{10} to a lesser extent, was detected to have the most important role in coking. For the example presented, more than 80% of the coke is originated from aromatic species. A_8 is mainly formed from 1-octene via cyclisation of alkenes followed by hydride transfer and deprotonation, vide Fig. 2, whereas A_{10} is predominantly formed out of *n*-decane. The alkylation of octenes and decanes also contributed appreciably to coking, in particular non-branched alkenes that are less susceptible to cracking and, hence, are more available for alkylations.

During the cracking of *methylcyclohexane/1-octene*, side chain alkylation of aromatics did not influence coking as also observed with *n*-decane/1-octene. Due to its large contribution in the reaction effluent, toluene was found to importantly contribute to coking via nucleus alkylation, for the given example in Fig. 8, more than 75% of the formed coke is originated from toluene. Other aromatics, i.e., benzene, xylenes and A_9, also contribute to coke, in particular xylenes. The latter is produced not only out of toluene via disproportionation but also out of 1-octene via cyclisation and hydride/deprotonation steps, cfr. Fig. 2. Similarly as observed with *n*-decane/1-octene, the alkylation of non-branched octenes had a moderate contribution to coking.

In contrast to what has been observed for *n*-decane/1-octene and methylcyclohexane/1-octene, side chain alkylation of aromatics, in particular on A_{10}, contributes to coking when cracking *n-butylcyclohexane/1-octene,* vide Fig. 9. This is understandable based on the relatively higher proportion of heavier aromatics when cracking larger cycloalkanes. The nucleus alkylation of aromatics A_8–A_{10}, however, exhibits the highest contribution to coke as has also been observed for the other mixtures. Consistently to what has been observed for the two examples above, a moderate contribution of the alkylation of octenes to coke was observed, being lower than 20%, for the given example.

4. Conclusions

A SEMK model in the relumped form is able to describe the initial rates of coke formation during the catalytic cracking of (cyclo)alkane/1-octene mixtures by assuming three irreversible, rate-determining steps involving reversibly formed gas phase, i.e., monoaromatics, and surface coke precursors, i.e., aromatic carbenium ions. These three steps are:

1. side chain alkylation of phenyl substituted carbenium ions with small alkenes (C_3–C_5),
2. nucleus alkylation of aromatic components with small carbenium ions (C_3–C_5), and
3. alkylation of C_8–C_{10} alkylcarbenium ions with small alkenes (C_3–C_5)

The bulky alkylated products, i.e., species with a carbon number of at least 11 and a relatively high branching degree, can be considered as coke.

The values of activation energies obtained via non-isothermal regression of the experimental coking data reflect the fundamental character of the SEMK. The estimated values are feedstock independent and are in line with what can be expected from carbenium ion chemistry. For *n*-decane/1-octene cracking, the increase in rate coefficients with the temperature was overcompensated by a decrease in the surface coke precursors' concentrations, while for the other feedstocks used, the initial coking rates were increasing with the reaction temperature.

Nucleus alkylation followed by alkylation of relatively long acyclic carbenium ions has the most important contribution to coking while the side chain alkylation of aromatics carbenium ions is only important when relatively large aromatics are present in the gas phase.

The model's flexibility is such that opposite trends with the temperature observed for the various investigated feedstocks are qualitatively reproduced. Moreover, the SEMK model is constructed in such a way that its extension and application to industrial feedstocks is possible.

Acknowledgements

R. Quintana-Solórzano acknowledges Mexican Petroleum Institute for his grant. The authors thank TOTAL for providing the equilibrium catalyst as well as P. Beyney (TOTAL) for stimulating discussions. This research was partly carried out in the framework of the Interuniversity Attraction Poles Program funded by the Belgian Science Policy.

References

[1] M. Guisnet, P. Magnoux, D. Martin, in: C.H. Bartholomew, G.A. Fuentes (Eds.), Catalyst Deactivation, Vol. 53, Elsevier Science, Amsterdam, 1997 , p. 1.
[2] M. Guisnet, P. Magnoux, Catal. Today 36 (1997) 477.
[3] G.M. Bollas, I.A. Vasalos, A.A. Lappas, D.K. Iatridis, G.K. Tsioni, Ind. Eng. Chem. Res. 43 (2004) 3270.
[4] C.H. Bartolomew, Appl. Catal. A: Gen. 212 (2001) 17.
[5] B.W. Wojciechowski, Catal. Rev. Sci. Eng. 40–3 (1998) 209.
[6] G.F. Froment, in: C.H. Bartholomew, G.A. Fuentes (Eds.), Catalyst Deactivation, Vol. 53, Elsevier Science, Amsterdam, 1997, p. 53.
[7] H.B. Beirnaert, J.R. Alleman, G.B. Marin, Ind. Eng. Chem. Res. 40 (2001) 1337.
[8] M.F. Reyniers, H. Beirnaert, G.B. Marin, Appl. Catal. A: Gen. 202 (2000) 49.
[9] M.F. Reyniers, Y. Tang, G.B. Marin, Appl. Catal. A: Gen. 202 (2000) 65.
[10] R. Quintana-Solorzano, J.W. Thybaut, G.B. Marin, R. Lødeng, A. Holmen, Catal. Today 107–108 (2005) 619.
[11] M. Van Sint-Annaland, J.A.M. Kuipers, W.P.M. van Swaaij, Catal. Today 66 (2001) 427.
[12] G.B. Marin, J.M. Beeckman, G.F. Froment, J. Catal. 97 (1986) 416.
[13] R. Quintana-Solórzano, J.W. Thybaut, G.B. Marin, Appl. Catal. A: Gen. 314 (2006) 184.
[14] P. T. Boggs, R. H. Byrd, J. E. Rogers, R. B. Schnabel, ODRPACK V. 2.01 User's Reference Guide (1992). http://www.netlib.com.
[15] R. Quintana-Solorzano, J.W. Thybaut, G.B. Marin, Chem. Eng. Sci., (in press). doi:10.1016/j.ces.2007.01.008.
[16] L. R. Petzold, C. Hindmarsh, LSODA solver for ODE equations (1997). http://www.netlib.com
[17] Q. Chen, J.H.B.J. Hoebink, G.B. Marin, Ind. Eng. Chem. Res. 30 (1991) 2088.
[18] M.A. Baltanás, K.K. Van Raemdonck, G.F. Froment, S.R. Mohedas, Ind. Eng. Chem. Res. 28 (1989) 899.

[19] Y.V. Kissin, J. Catal. 146 (1994) 358.
[20] J.L. Figueiredo, M.L.G.O.M. Pinto, J.J.M. Orfao, Appl. Catal. A: Gen 104 (1993) 1.
[21] E. Vynckier, G.F. Froment, in: G. Astaritra, S.I. Sandler (Eds.), Kinetic and Thermodynamic Lumping of Multicomponent Mixtures, Vol.10, Elsevier Science, Amsterdam, 1991, p. 131.
[22] N.V. Dewachtere, F. Santaella, G.F. Froment, Chem. Eng. Sci. 54 (1999) 3653.
[23] W.A. Groten, B.W. Wojciechowski, J. Catal. 122 (1990) 326.
[24] G. Yaluris, J. Catal. 153 (1995) 54.
[25] J.A. Dumesic, F.D. Rudd, L.M. Aparicio, J.E. Rekoske, A.A. Treviño, The Microkinetics of Heterogeneous Catalysis, ACS Professional Reference Book, Washington DC, 1993.
[26] G. Martens, G.B. Marin, J.A. Martens, P. Jacobs, G.V. Baron, J. Catal. 195 (2000) 253.
[27] A.A. Brillis, G. Manos, Ind. Eng. Chem. Res. 42 (2003) 2292.